Applied Catalysis B: Environmental 163 (2015) 584–590

Contents lists available at ScienceDirect

Applied Catalysis B: Environmental

journal homepage: www.elsevier.com/locate/apcatb

Solar conversion of seawater uranium (VI) using TiO_2 electrodes

Young Kwang Kim [a], Seunghoon Lee [b], Jungho Ryu [c], Hyunwoong Park [b,*]

[a] Department of Physics, Kyungpook National University, Daegu 702-701, Republic of Korea
[b] School of Energy Engineering, Kyungpook National University, Daegu 702-701, Republic of Korea
[c] Mineral Resources Research Division, Korea Institute of Geoscience and Mineral Resources, Daejeon 305-350, Republic of Korea

ARTICLE INFO

Article history:
Received 11 June 2014
Received in revised form 19 August 2014
Accepted 23 August 2014
Available online 2 September 2014

Keywords:
Photocatalytic
Metal reduction
Superoxide
Nuclear wastes
Solar energy

ABSTRACT

Uranium(VI) spiked in natural seawater was photoelectrochemically reduced using porous TiO_2 film electrodes at varying potential biases (E_{bias}s) and pH values. Linear sweep voltammograms of TiO_2 electrodes in seawater with U(VI) at pH 8.2 exhibited the characteristic reduction peaks at $-0.95\,V_{SCE}$ and anodic peaks at $-0.75\,V_{SCE}$. These peaks shifted anodically and became less pronounced with decreasing pH values from 8.2 to 3. At the natural seawater pH of 8.2, photoelectrochemical (PEC) treatment ($E_{bias} = -1.0\,V_{SCE}$; AM 1.5 G) was found to be considerably more effective in reducing U(VI) than photocatalytic (PC) treatment (without E_{bias}) and electrochemical (EC) treatment (without irradiation), and even the combination of the two treatment processes. The synergistic effect of the PEC U(VI) reduction varied depending on the E_{bias}s and pH values, and was further confirmed by the Faradaic efficiency (ε), which was close to 100%. Inductively coupled plasma spectroscopy (ICP) and detailed surface analyses of the TiO_2 using various techniques (TEM/EDX, SEM/EDX, and XPS) indicated that ~95% of uranium in the PEC-treated experiment was adsorbed on TiO_2 with 57% as $U^{4.6+}$ and 14% as U^{4+}, whereas ~98% of uranium in the EC-treated experiment remained in solution, containing 62% as $U^{4.6+}$ and 12% as U^{4+}. Under certain conditions (e.g., at a pH of 3.0 and/or with N_2-purging), no reduction of U(VI) was observed irrespective of the E_{bias} and irradiation. To further investigate the observed lack of U(VI) reduction, surface chemistry and energetics between TiO_2 and U(VI) were studied as a function of pH. Finally, a role of superoxide radicals as an electron shuttle between TiO_2 and U(VI) was established as a primary U(VI) reduction mechanism.

1. Introduction

Nuclear power is a carbon-free energy source, which can contribute to the reduction of anthropogenic CO_2 emissions by ~6% of the total amount of carbon emitted from the use of fossil fuels [1–3]. Currently, there are two major challenges for sustainable nuclear power generation. First, uranium needs to be continuously and securely supplied at reasonable prices. Uranium is a relatively common element, yet highly localized in the Earth's crust [3–5]; hence its continuous supply needs to be guaranteed in terms of energy security. Second, the environmental impact from the operation of nuclear power plants needs to be minimized [1,2]. Unfortunately, the operational safety of nuclear power plants and the radiological hazard associated with spent nuclear fuel are of great public concern, following the Hanford and the Fukushima nuclear accidents. Particularly, the ambient radioactivity concentration of seawater near the Fukushima nuclear plant increased a few thousand times above the permissible regulatory limit [6]. Although both spent fuels and leaked fissile nuclides can be isolated in geological repositories, however, there are no such repositories in operation [1].

In this regard, the extraction of dissolved uranium (uranyl) from natural seawater and the recovery of accidentally released radioactive nuclides (actinides, Cs, etc.) from nuclear power plants to the surrounding ocean need to be investigated. The natural uranium concentration in seawater is as low as 3 ppb [3], requiring long collection periods of several months to years with a large quantity of adsorbents (e.g., amidoximes) [7]. However, in the case of nuclear accidental releases of radioactive nuclides to the ocean, the ambient seawater uranium concentration can increase significantly. It has been shown that hexavalent uranium (U^{6+}) can be physically removed by adsorption using hydrous [8,9] or crystallized oxides [10,11], polymers [7,12], or sediment [13], and/or reduced to U^{4+} (e.g., UO_2) biologically [14,15], chemically [16,17], and photocatalytically [18–22]. Despite some uranium recovery tests in seawater [7,8,12], however, no attempt has been made for

* Corresponding author. Tel.: +82 53 950 8973; fax: +82 950 8979.
E-mail address: hwp@knu.ac.kr (H. Park).

http://dx.doi.org/10.1016/j.apcatb.2014.08.041
0926-3373/

direct reduction of U^{6+} in seawater. Seawater is a complex matrix containing various inorganic ions, such as Cl^-, Na^+, Mg^{2+}, SO_4^{2-}, Ca^{2+}, K^+, etc. [23], which can interfere with U^{6+} reduction, making the redox chemistry complicated.

For the reduction of seawater hexavalent uranium, a photoelectrochemical approach can be employed using TiO_2 electrodes under simulated sunlight [24,25]. Only a few studies have reported that irradiated TiO_2 particles are capable of reducing U(VI) in well-defined solutions (mostly ultra-pure water) [18,21,22,26]. The maximum adsorption capacity of commercially available TiO_2 particles (e.g., Degussa P25) for uranyl ions, $(UO_2)_m(OH)_n^{2m-n}$, was estimated to be 0.3 g/g-TiO_2 at a pH of ~7 [18]. Under ultraviolet (UV) irradiation, uranyl was shown to be reduced to tetravalent uranium [19], while the photoreduction occurred only for adsorbed uranium species on the TiO_2 [22]. Dissolved oxygen appeared to interfere with the photoreduction and even re-oxidized the reduced tetravalent uranium adsorbed on the TiO_2 [21]. Aqueous organics such as humic acid [27], EDTA [21], and formate [18,28] were shown to further complicate the photocatalytic uranium reduction process due to precipitation and complexation with uranium.

To the best of our knowledge, this is the first study for the conversion of seawater uranium(VI) by irradiated TiO_2 electrodes. The conventional suspension-type photocatalytic reduction of hexavalent uranium was demonstrated only in distilled water, yet very limited reduction was observed in the absence of hole scavengers due to rapid charge recombination [18,21]. The photocatalytic process in seawater is challenging. Seawater has diverse interfering inorganic ions present in high concentrations, highly limiting the photocatalytic activity, compared to non-saline water [29]. However, when the photoelectrochemical treatment is applied to the TiO_2 film electrodes, total uranium reduction was observed on the TiO_2 surface under simulated sunlight conditions without any supporting electrolyte or hole scavengers. This study found that there is an optimal potential for hexavalent uranium reduction and that the photoelectrochemical treatment induces synergistic effects on the seawater uranium reduction kinetics, compared to the photocatalytic and electrochemical treatments. Surface analysis of TiO_2 using various techniques such as SEM, TEM, EDX, XPS, etc., confirmed the reduction of U^{6+} to U^{4+} and $U^{4.6+}$.

2. Experimental

2.1. Reagents and materials

Uranyl nitrate ($UO_2(NO_3)_2$•$6H_2O$, purity >98.0%, Sigma–Aldrich), arsenazo III ($(HO)_2C_{10}H_2(SO_3H)_2(N{=}NC_6H_4AsO_3H_2)_2$, Sigma–Aldrich), and perchloric acid ($HClO_4$, 70%, Daejung) were used as received. Stock solutions of U(VI) (100 ppm) were prepared weekly by dissolving uranyl nitrate in natural seawater derived from the East Sea, Korea (latitude: 36.13°, longitude: 129.40°). Prior to use, the sampled seawater was filtered with 0.45-μm PTFE membranes (Millipore) to remove particulate matter. For fabrication of TiO_2 film electrodes, commercially available TiO_2 powders (Degussa P25 with a primary particle size of ~30 nm; anatase and rutile mixture in the ratio of 8:2, BET surface area of ~50 m^2/g) were mixed with aqueous polyethylene glycol (PEG) solution in the ratio of TiO_2:PEG = 0.18:1 by weight [25,30]. As-prepared TiO_2 paste was spread on fluorine-doped, tin oxide-coated (F:SnO_2) glass (FTO, Pilkington, 3 mm thick) (1.5 cm × 3.5 cm), masked with 3 M adhesive tape as spacers (thickness of ca. 0.048 mm). After drying in air, the TiO_2 electrodes were annealed at 500 °C for 30 min to remove the PEG and obtain firm contact of porous TiO_2 film to the FTO (Fig. S10). The film thickness was approximately 9 μm, while the amount of TiO_2 in the coating was estimated to be 10(±0.23) mg, or 1.9 mg cm^{-2}. As an effective adsorbent of uranium in seawater, hydrous titania (TiO_2•xH_2O or $Ti(OH)_x$) with a high surface area (>300 m^2/g) was prepared by following literature [9,10,31]. In brief, 10 mL of titanium tetra-isopropoxide (98%, Junsei) was mixed with 300 mL of 2-propanol (HPLC grade, Fisher Scientific) and vigorously stirred in an ice bath (<4 °C). Then, 90 mL of acetic acid (99.7%, Sigma–Aldrich) was slowly added, followed by the addition of distilled water (0.5 mL) to the stirred mixture. A clear, slightly yellowish solution was obtained, which was dried at room temperature, followed by washing several times with distilled water and finally collected as a powder.

2.2. Photoelectrochemical uranium reduction

The photoelectrochemical (PEC) study was performed using a three-electrode system in natural seawater (50 mL) spiked with 100 ppm (420 μM) of uranyl ions. A TiO_2 electrode (0.785 cm^2 in contact), saturated calomel electrode (SCE), and graphite were used as a working, reference, and counter electrodes, respectively. The standard mean chemical composition of seawater (salinity: 35 g·kg^{-1}) is well documented (Table S1) [23]. A 150-W Xenon arc lamp (ABET Tech.) equipped with an AM1.5 G filter was used as a light source with a light intensity of 400 mW cm^{-2}. Light was irradiated to the backside of the TiO_2 electrodes (FTO side). To examine the redox characteristics of TiO_2 in seawater as a function of uranyl concentration (0–100 ppm) at different pH values (8.2, 6, or 3), cyclic potential sweeps were applied between +1.5 (starting and ending potential) and −1.5 V_{SCE} (reversal potential) at a scan rate of 10 mV s^{-1} in the absence or presence of light. In addition, constant potentials (−0.4, −0.7, and −1.0 V_{SCE}) were applied to the TiO_2 electrodes to photoelectrochemically reduce uranium at varying pH values. During these potentiostatic modes, solutions of 0.5 mL were sampled every 30 min for uranium analysis while currents were recorded. For comparison, either AM1.5 G light was irradiated to TiO_2 without any potential bias (photocatalytic, PC) or constant potential biases were applied to TiO_2 in the absence of light (electrochemical, EC).

2.3. Measurement of seawater uranium

A spectrophotometric method for uranium was employed with arsenazo III as a chelating indicator of U(VI). This method has been shown to be highly selective for hexavalent uranium [32,33] and reliable, with no interference from seawater ions [34–36]. 20 mg of arsenazo III was dissolved in 100 mL of aqueous perchloric acid solution (3 M) using ultrasonic treatment for 30 min. This indicator solution was mixed with U(VI) stock or U(VI) sample solutions in a 5:1 volumetric ratio (equivalent to 2:1 molar ratio) for 6 min, and then analyzed with a UV-Vis spectrophotometer (PG Instrument). Free arsenazo III exhibited an absorption band at 539 nm, whereas arsenazo III with U(VI) displayed two absorption bands at 605 nm and 653 nm due to complexation (Fig. S1). The intensities of these absorption bands were proportional to U(VI) concentration in the range of up to 30–40 ppm at pH values of interest. The amounts of total uranium were also determined by inductively coupled plasma spectroscopy (ICP) (Perkin Elmer, Optima 7300DV). The ICP standard solution of uranium (1000 ± 10 ppm, GFS Chemicals) in 5% nitric acid was used for the measurements.

2.4. Surface analysis

After the PEC treatment of uranium (100 ppm) for 3 h, TiO_2 particles were sampled from the electrodes, and their surface morphology and composition were analyzed using a high-resolution transmission electron microscope (HR-TEM, Hitachi, HF-3300)

equipped with an energy dispersive X-ray (EDX) spectrometer. Copper grid (Ted pella, Inc, Pelco 300 mesh, 3.0 mm O.D.) was used for the TEM analysis. The TiO_2 film electrodes were also examined with a scanning electron microscope (SEM, Hitachi, SU-8020) equipped with an EDX spectrometer. The elemental binding energies and oxidation states of the TiO_2 samples used for uranium removal were determined using an X-ray photoelectron spectroscope (Thermo Fisher Scientific, Theta Probe AR-XPS System) fitted with monochromated Al Kα source ($h\nu$ = 1486.6 eV). The anode was operated at 150 W (15 kV, 10 mA).

2.5. Modeling of uranium species distribution in seawater

The species distributions of U(VI) and titanol surface groups (>Ti-OH) in seawater were calculated using the MINEQL software (version 4.6). For the species distribution calculation of U(VI), the input variables were U(VI) (4.2×10^{-4} M), $pCO_2 = 10^{-3.5}$ bar, ionic concentrations of seawater components (Table S1), 25 °C, and 1 atm. The distribution of >Ti-OH was calculated using the values pKa_1 = 3.8 and pKa_2 = 8.7. The input variables were TiO_2 at 1 g L^{-1} (1.2×10^{-2} M), 25 °C, and 1 atm. Ionic strength was automatically calculated.

3. Results and discussion

3.1. Interaction of TiO_2 and seawater uranium

Fig. 1a shows the cyclic voltammograms of TiO_2 electrodes in natural seawater in the absence and presence of varying concentrations of U(VI) ions at pH 8.2. In the absence of U(VI), no distinct cathodic peak was detected; however, a significantly large anodic peak at ca. −1.2 V_{SCE} was observed. The anodic peak resulted from non-Faradaic processes (e.g., charging/discharging and/or cation (Na^+, H^+, etc.) filling/removing in TiO_2), which are often reported in other common electrolytes (e.g., Na_2SO_4) [25,37,38]. Small peaks at −0.5 and 0 V_{SCE} were not always detected (Fig. S2), which can be attributed to the presence of trace elements or components in seawater. In the presence of U(VI), additional reduction peaks at −0.95 V_{SCE} and anodic peaks at −0.75 V_{SCE} were observed irrespective of the U(VI) concentration. The reduction peaks are presumed to be related to the one-electron reduction of U(VI) (e.g., UO_2^{2+}, reaction (1)) [39].

$$U^{VI}O_2^{2+} + e^- \rightarrow U^{V}O_2^{+} \quad (1)$$

The magnitude of the cathodic peaks was greater than that of the corresponding anodic peaks, indicating that the redox behavior of U(VI) is quasi-reversible. Once produced, the pentavalent uranium ($U^{V}O_2^{+}$) disproportionate to U^{6+} and U^{4+} (reaction (2)).

$$2U^{V}O_2^{+} + 4H^+ \rightarrow U^{4+} + U^{VI}O_2^{2+} + 2H_2O \quad (2)$$

Insignificant increase in the magnitude of the cathodic peaks with increasing U(VI) concentrations further suggests that the exposed TiO_2 surface (ca. 0.785 cm^2) was fully occupied by uranium ions at 25 ppm (equivalent to 5.25 μmol). This speculation is reasonable because the number of uranium molecules at 25 ppm (~9.5×10^{17} U atoms) is comparable to that of the surface titanol groups (>Ti-OH) (~3×10^{17} Ti atoms, assuming 4 titanol groups per 1 nm × 1 nm TiO_2 surface [24] at 1.5 mg-TiO_2 with a surface area of 50 m^2/g in contact with the uranium solution).

Fig. 1b shows the pH-dependent changes in the cyclic voltammograms of TiO_2 electrodes in natural seawater without and with 100 ppm U(VI). The overall shapes and peak positions of voltammograms in uranium-free seawater were hardly affected with pH change. In the presence of uranium, however, the characteristic redox peaks gradually shifted anodically with decreasing pH. The reduction peaks at pH values of 8.2, 6, and 3 were observed at approximately −0.95, −0.8, and −0.35 V_{SCE}, respectively, while the oxidation peaks were located at −0.7, −0.65, −0.57 V_{SCE}, respectively. It should be noted that the magnitude of the redox peaks decreased with decreasing pH values, presumably due to an increase in the electrostatic repulsion of TiO_2 and U(VI).

The effects of pH on the speciation of U(VI) and TiO_2 were investigated in seawater using the MINEQL software to examine the pH-dependent electrostatic interaction of TiO_2 and U(VI). As shown in Fig. 2a, the primary U(VI) species are UO_2^{2+}, UO_2Cl^+, and UO_2F^+ at pH < 4. The former species was often identified as a single species at pH < 4 in freshwater [40], whereas the latter two species were found to be relatively abundant in seawater due to the high concentrations of chlorides (ca. 0.55 M, $K_{eq} = 10^{0.17}$ M^{-1}) [41] and fluorides (ca. 7×10^{-5} M, $K_{eq} = 10^{5.16}$ M^{-1}) [23,41]. At pH 5–6, UO_2^{2+} is hydrolyzed to mostly $(UO_2)_2(OH)_2^{2+}$ and $(UO_2)_3(OH)_5^+$, and further transformed into hydroxyl-carbonated species such as $(UO_2)_2(OH)_3CO_3^-$ in the presence of dissolved CO_2 (ca. 1×10^{-5} M), bicarbonate (ca. 1.83×10^{-3} M), and carbonate (ca. 2.7×10^{-4} M) [5,20,40]. At pH > 7, carbonate species dominate the uranium chemistry, forming $UO_2(CO_3)_2^{2-}$ and $UO_2(CO_3)_3^{4-}$. Meanwhile, the surface titanol groups of TiO_2 particles are predominantly >Ti-OH_2^+ (~89%) at pH 3 and >Ti-OH (~98%) at pH 6, while >Ti-OH (~70%) and >Ti-O^- (~30%) are present together at pH 8.2 [42]. Accordingly, the electrostatic repulsions between TiO_2 and U(VI) species at pH 3 must be very strong (Fig. 2b, case I), hindering U(VI) ions interaction with TiO_2, thereby inhibiting direct electron transfer. This was confirmed by lack of adsorption of U(VI) on TiO_2 particles and the presence of small redox peaks at pH 3. On the other hand, the amount of U(VI) adsorbed on the TiO_2 electrodes at pH 6 was found to be ~9 ppm. It appears that the >Ti-OH groups undergo

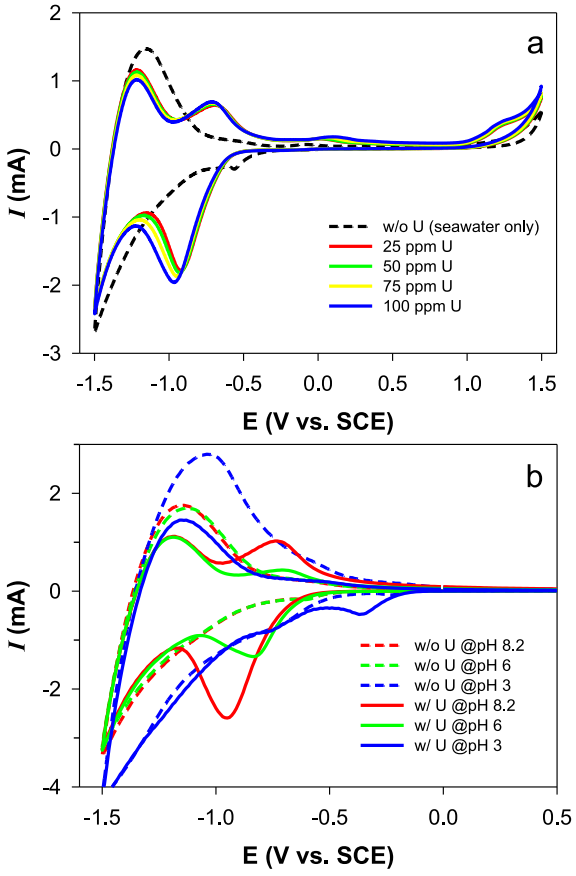

Fig. 1. Cyclic voltammograms of TiO_2 electrodes in seawater with (a) varying concentrations of U(VI) at pH 8.2 and (b) 100 ppm uranium(VI) at varying pH values; air-equilibrated.

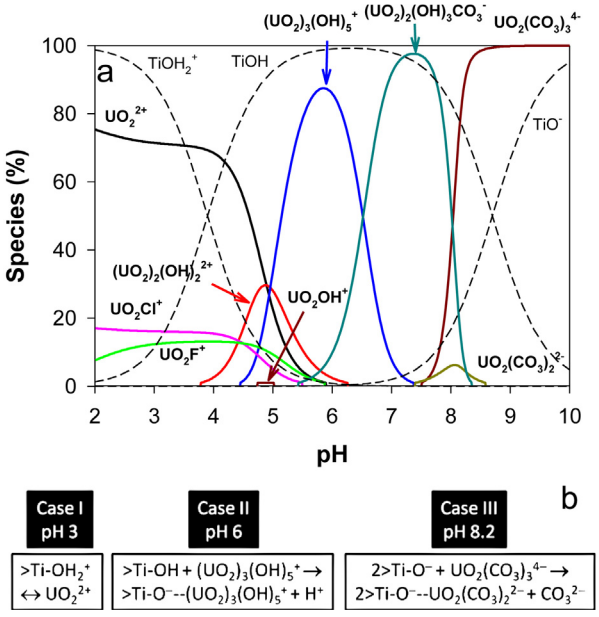

Fig. 2. (a) pH-dependent speciation of U(VI) (solid lines) and surface titanol groups (>Ti-OH) (broken lines) in seawater calculated with MINEQL software. [U(VI)] = 100 ppm (4.2×10^{-4} M); [TiO_2] = 1 g L^{-1}; $pCO_2 = 10^{-3.5}$ bar; concentration of natural seawater components shown in Table S1; 25 °C; 1 atm. Ionic strength automatically calculated. (b) Interactions of U(VI) and TiO_2 at varying pH values.

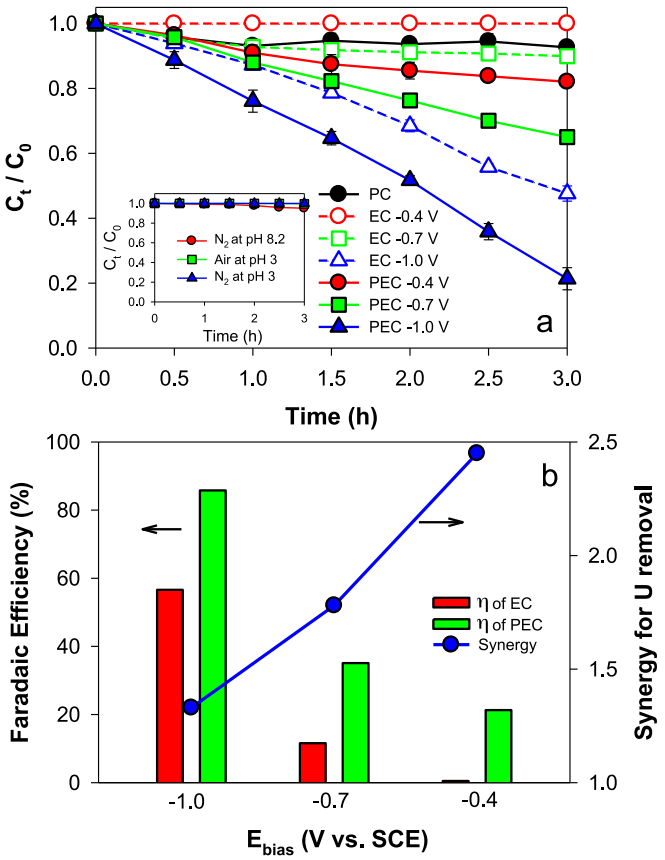

Fig. 3. (a) Time-profiled changes in U(VI) concentrations during the photocatalytic (PC, irradiation only), electrochemical (EC, bias only), and photoelectrochemical (PEC, irradiation + bias) treatment of 100 ppm U(VI) in seawater at pH 8.2. Inset shows the effects of N_2-purging and pH on the time-profiled changes in U(VI) concentrations. (b) Faradic efficiencies (ε) and synergy factor ($\Delta U_{PEC}/(\Delta U_{EC} + \Delta U_{PC}) \times 100\%$) for the reduction of U(VI) to U(IV) in EC and PEC treatment of U(VI) in seawater at pH 8.2. AM 1.5 G (400 mW cm^{-2}); air-equilibrated.

proton exchange with $(UO_2)_3(OH)_5^+$ (case II) [11,43]. At pH 8.2, the amount of U(VI) adsorbed was ~1.6 ppm. It is of note that the two >TiO^- groups participate in a complexation reaction with a single $UO_2(CO_3)_3^{4-}$ (case III) [44,45]. Because the fraction of >TiO^- groups is only 30% at this pH value, the amount of U(VI) adsorbed may not be large. As the pH was increased to 9.6, at which the >TiO^- groups are predominant at >80%, the amount of U(VI) adsorbed also increased to ~8 ppm. This supports the model in case III.

3.2. Photoelectrochemical U(VI) removal

Fig. 3a shows time-profiled changes in U(VI) concentrations (C_t/C_0) when TiO_2 was irradiated without bias (photocatalytic; PC), and biased at varying potentials (E_{bias} = −0.4, −0.7, and −1.0 V_{SCE}) without (electrochemical; EC) and with irradiation (photoelectrochemical; PEC) at pH 8.2. Under PC treatment conditions, approximately U(VI) of 10 ppm was removed. Application of E_{bias} was found to increase U(VI) removal, which was significantly accelerated by simultaneous irradiation. There were obvious synergistic PEC effects on U(VI) removal at all three E_{bias}s. For example, EC treatment (E_{bias} = −1.0 V_{SCE}) for 3 h removed U(VI) concentration by approximately 50 ppm, whereas PEC treatment for the same period at −1.0 V_{SCE} removed the U(VI) concentration by about 80 ppm. Hence, the synergistic effect at −1.0 V_{SCE} was ca. 130% ($\Delta U_{PEC}/(\Delta U_{EC} + \Delta U_{PC}) \times 100\%$). The synergistic effects increased to 180% and 250% at −0.7 and −0.4 V_{SCE}, respectively (Fig. 3b). The greatest synergy at −0.4 V_{SCE} was attributed to zero ΔU_{EC} (Fig. 3a; see the next section for discussion), while the largest removal of uranium at −1.0 V_{SCE} was attributed to the match between the cathodic peak and the potential biased (Fig. 1a). The importance of the potential match was confirmed at pH 6, where E_{bias} at −0.7 V_{SCE} was more effective than the other two E_{bias}s in terms of PEC U(VI) removal (Fig. S3). A comparison of Faradaic efficiencies (ε) for uranium removal also shows the synergistic effect of PEC treatment (Fig. 3b and Fig. S4). For the estimation of ε, a two-electron reduction was assumed (reactions (1) and (2); see below for more accurate estimation). It was found that ε_{PEC} is always higher than ε_{EC} and the difference becomes greater with decreasing E_{bias} primarily due to low ε_{EC} at small E_{bias}. It should be noted that, at a small E_{bias}, a thick TiO_2 film (~9 μm) behaves like an insulator with few charge carriers in the absence of irradiation. Upon irradiation, however, even a small E_{bias} can drive effective separation of the photogenerated charges ($\varepsilon_{PEC@-0.7\,V} \sim 35\%$) that would recombine in the absence of E_{bias} ($\varepsilon_{EC@-0.7\,V} \sim 10\%$). As E_{bias} increased, ε_{EC} increased five-fold ($\varepsilon_{EC@-1.0\,V} \sim 50\%$) while ε_{PEC} increased only by 1.5 times due to the saturated charge separation effect beyond a critical potential.

The removed uranium was found to be partitioned between the TiO_2 surface and the solution. ICP analysis indicated that ~95% and ~10% of the total uranium were adsorbed on PEC- and PC-treated TiO_2 samples, respectively, whereas ~98% of the total uranium remained in solution under EC-treated conditions (Fig. S5). A comparison of this result with the results depicted in Fig. 3a suggests that most of the U(VI) reduced was simultaneously adsorbed on the TiO_2 surface under PC and PEC treatment conditions, whereas under EC conditions, the reduced uranium remained in solution, showing no significant adsorption. The observed difference in the adsorption behavior can be attributed presumably to the photocharging effect of TiO_2. At E_{bias} without irradiation, the substrate (FTO) is electrically biased, while most of the thick TiO_2 film is less charged due to its insulating property. On the other hand, irradiation makes all TiO_2 particles generate charge carriers and the charged TiO_2 layer becomes active in the interfacial binding of uranium ions. Alternatively, the characteristics of TiO_2 surface charge

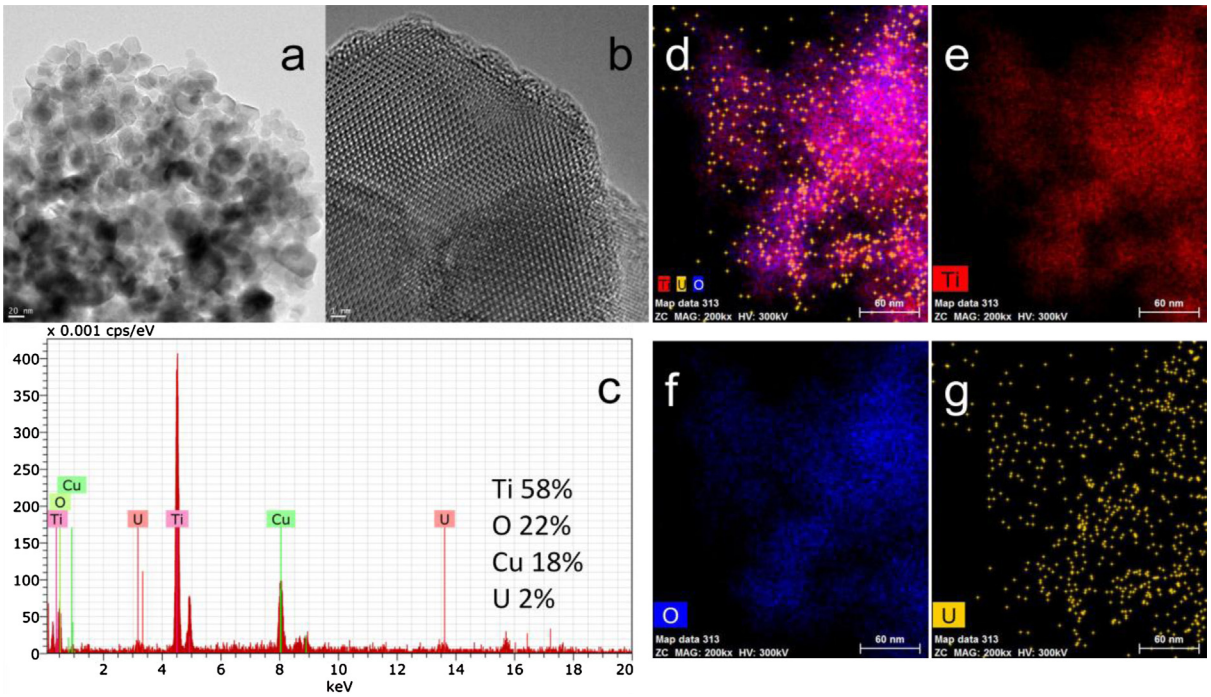

Fig. 4. (a, b) HR-TEM, (c) EDX, and (d–g) elemental mapping analyses of TiO_2 surface after PEC treatment of 100 ppm U(VI) in seawater (pH 8.2) at $-1.0\,V_{SCE}$ for 3 h. AM 1.5 G ($400\,mW\,cm^{-2}$); air-equilibrated.

under EC and PEC conditions could be different [46]. A detailed investigation on the different interactions between EC and PEC treatments will be carried out later. From a practical point of view, however, the PEC treatment is very promising in efficient U(VI) removal, as well as in the effective recovery of uranium from seawater.

In order to verify the uranium adsorbed on the TiO_2 surface, TiO_2 particles were collected from FTO following PEC treatment of 100 ppm U(VI) solution for 3 h, and then subjected to HR-TEM and EDX elemental mapping analysis (Fig. 4). The collected TiO_2 particles had a similar morphology as the fresh particles of primary particle size 20–30 nm and the crystalline structure remained intact (Fig. 4a and b). No visible evidence of uranium deposition was found on TiO_2 particles. The EDX analysis results, however, showed the presence of uranium at 2 atomic % on TiO_2 surface (Fig. 4c). The presence of Cu in the EDX analysis was attributed to the Cu grid used as a support. The EDX elemental mapping further indicated that the uranium is uniformly distributed on the entire TiO_2 sample surface (Fig. 4d–g). The uniform distribution of uranium on the TiO_2 film electrode was also confirmed by SEM analysis with EDX elemental mapping (Fig. S6). In this analysis, TiO_2 particles were not collected. Similar to the TEM-EDX mapping results, uranium was found to be distributed well on the TiO_2 surface and the bulk of the film, and its amount was approximately 6 atomic % (Fig. S7). Furthermore, the cross-sectional view of ca. 9 μm-thick TiO_2 film clearly indicates the uniform distribution of uranium throughout the entire TiO_2 film (Fig. S6e). This suggests that U(VI) ions penetrated into the porous TiO_2 film and subsequently reduced photoelectrochemically.

The TiO_2 particles used for PC, EC, and PEC treatments of U(VI) were collected and analyzed with XPS to examine the chemical states of the uranium ions at the TiO_2 surface (Fig. 5). Note that the actual uranium species at dried TiO_2 samples may be different from those at wet TiO_2 due to dehydration and structural change. However, the oxidation states of the uranium species should be unchanged by the dehydration. The overall spectral shapes of U4f band were similar for the three PC-, EC-, and PEC-treated TiO_2 samples, except for (1) the band shifts for EC- and PEC-treated

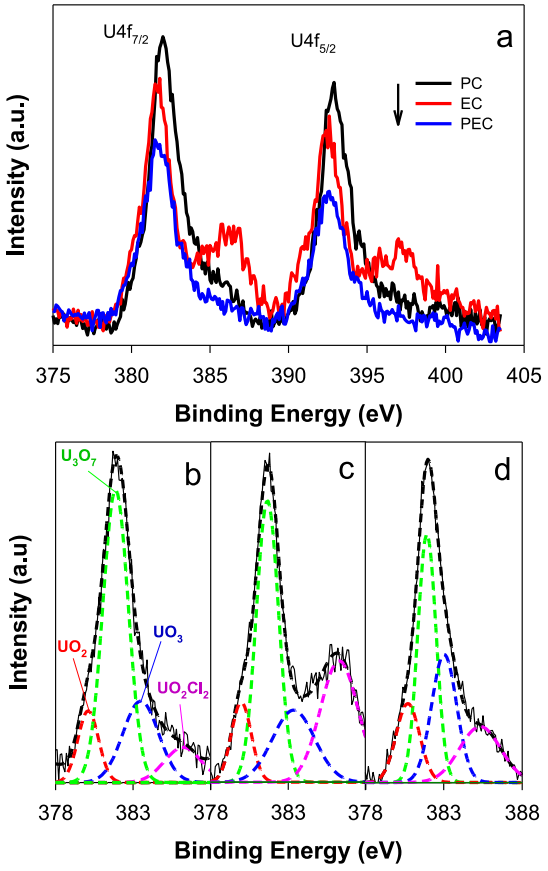

Fig. 5. (a) XPS analysis of TiO_2 surface after PC, EC, and PEC treatments of U(VI) in seawater. (b–d) Deconvoluted $U4f_{7/2}$ bands ((b) PEC, (c) EC, (d) PC). See Fig. 4 for experimental condition.

Table 1
Distributions of uranium species between TiO_2 surfaces and in solutions following photocatalytic (PC), electrochemical (EC), and photoelectrochemical (PEC) treatments of U(VI) in seawater for 3 h[a].

Species[b]	U oxidation state[b]	PC (%)		EC (%)		PEC (%)	
		Surface[c] (10%)	Solution[c] (90%)	Surface (2%)	Solution (98%)	Surface (95%)	Solution (5%)
UO_3	+6	25	26	29	23	21	23
UO_2Cl_2	+6	16	5	23	3	9	13
U_3O_7	+14/3	47	61	33	62	57	51
UO_2	+4	12	7	15	12	14	12
Sum[d]		100	100	100	100	100	100

[a] $[U(VI)]_0 = 100$ ppm; $E_{bias} = -1.0\ V_{SCE}$; AM1.5 G light (400 mW cm^{-2}); air-equilibrated.
[b] The percentage of each species (dried states) either on surface or in solution was estimated by XPS.
[c] Relative fraction of uranium distributed between surfaces and solutions. The amounts of total uranium remaining in solutions were analyzed by ICP; the difference was assumed to be located on the TiO_2 surface.
[d] Sum of species percentages either on surface or in solution. Hence, the actual amount of a species (e.g., UO_2 under PEC condition) could be estimated by following: $(0.14 \times 0.95)_{surface} \times 100$ ppm + $(0.12 \times 0.05)_{solution} \times 100$ ppm = 13.9 ppm.

TiO_2 samples to lower binding energy by ca. 0.4 eV and (2) a new shoulder ($U4f_{7/2}$ = ~386 eV) at EC-treated TiO_2 sample. The former suggests that EC and PEC treatments reduce U(VI) chemically more compared to PC treatment due to additional E_{bias}, while the latter appears to arise solely from the E_{bias}, not being related to photoeffect. The $U4f_{7/2}$ bands were further resolved to assess quantitatively the removed uranium species (Fig. 6b–d). Four major ionic species were identified as follows: UO_3 (383.5 eV), UO_2Cl_2 (386.2 eV), U_3O_7 (381.9 eV), and UO_2 (380.1 eV). Despite the similarities in the uranium species, their relative percentages were different from one another (Table 1). In PC- and PEC-treated samples, the fraction of U_3O_7 was the largest, followed by $UO_3 > UO_2 \sim UO_2Cl_2$. On the other hand, UO_3 and UO_2 were relatively abundant in the EC-treated sample.

The uranium remaining in solution was also analyzed using XPS. In order to collect the uranium in solution, hydrous titania particles ($TiO_2{\bullet}xH_2O$ or $Ti(OH)_x$) [31] with a high surface area (>300 m^2/g) were prepared following a procedure reported in the literature [9,10,31]. The adsorption capacity of hydrous titania for dissolved uranium was found to exceed 50 wt% and hence the species of all remaining uranium could be identified. The uranium ionic species distribution between on the TiO_2 surface and in the solution of the various samples subjected to different treatments was very similar (particularly for the PEC-treated samples) (Fig. S8 and Table 1). However, a remarkable difference was observed with the UO_2Cl_2 species in the EC-treated sample: 23% of uranium at surface (0.46% on the 2%-basis) versus 3% of uranium in solution (2.94% on the 98%-basis), which suggests that this species was formed on the TiO_2 surface electrically. For the PEC-treated sample, Faradaic efficiencies were re-calculated based on the estimated amounts of U_3O_7 (100 ppm × (0.57 × 0.95 + 0.51 × 0.05) = 56.7 ppm) and UO_2 species (100 ppm × (0.14 × 0.95 + 0.12 × 0.05) = 13.9 ppm), which were 102, 49, and 30% at −1.0, −0.7, and $-0.4\ V_{SCE}$, respectively.

3.3. U(VI) removal mechanism

Several conditions unfavorable for U(VI) removal were identified. For example, (1) hexavalent uranium in air-equilibrated seawater was not removed at pH 3 under all conditions irrespective of the E_{bias} (Fig. 3a inset and Table S2); (2) under EC treatment at $-0.4\ V_{SCE}$ and pH 8.2 no uranium removal was observed (Fig. 3a); and (3) the removal of dissolved oxygen by N_2-purging significantly inhibited the degree of uranium removal under all conditions (PC, EC, and PEC treatments), irrespective of the E_{bias} (Fig. 3a inset and Table S2). Note that N_2-purging had no significant effect on the pH (less than 0.1 unit) as well as on the voltammograms of seawater containing U(VI) (Fig. S9). To understand this intriguing behavior of uranium, the energy level of TiO_2 conduction band (CB) and the reduction potentials of U(VI) were compared as a function of E_{bias} (Scheme 1). According to this scheme, the photogenerated electrons could be directly transferred from the TiO_2 CB to U(VI) due to the energy difference ($|E_{CB} - E(U^{6+}/U^{4+})|$) of ~0.67 V. Even in the absence of irradiation, U(VI) could be reduced electrochemically at all three E_{bias}s. However, such an energy level-dependent charge transfer does not satisfactorily explain the aforementioned observations, especially (2) and (3). Alternatively, the adsorption of uranium could influence uranium removal. According to the adsorption model (Fig. 2), lack of U removal at pH 3 could be attributed to strong electrostatic repulsion between UO_2^{2+} and $>Ti\text{-}OH_2^+$. In addition, the photoelectrochemical simultaneous reduction and adsorption of uranium at pH 8.2 (Fig. 3a vs. Fig. S5) may support this model. However, this model could not explain the N_2-purging effects at all pH values because the U(VI) adsorption was not influenced by the N_2-purging.

Herein, we presume that dissolved oxygen plays a role of electron shuttle between TiO_2 and U(VI) (reactions (3) and (4)).

$$O_2 + e^- \rightarrow O_2^- \quad (3)$$

$$xO_2^- + U^{6+} \rightarrow U^{(6-x)+} + xO_2 \quad (4)$$

According to this mechanism, no uranium removal under EC treatment at $-0.4\ V_{SCE}$ (Fig. 3a) could be understood because oxygen is not electrochemically reduced at the E_{bias} (Scheme 1). No uranium removal with N_2-purging can be explained as well. Finally, the inactivity of TiO_2 electrodes in the removal of uranium at pH 3 also could be explained in terms of hydroperoxyl/superoxide radical chemistry. At pH 3, the formation of O_2^- (reaction (3)) is highly limited due to $pK_a(HO_2)$ of 4.8 [47]. HO_2 can also reduce U(VI). However, the possibility is very low because the reaction rates of metal ions (e.g., Cu^{2+}) with HO_2 are generally an order of magnitude slower than that with O_2^- [47]. In addition, HO_2 forms a dioxouranium(VI)–hydroperoxy complex upon reaction with UO_2^{2+} (reaction (5)) [47–49]. The addition of another HO_2 to the complex regenerates UO_2^{2+} with the formation of a hydroperoxyl

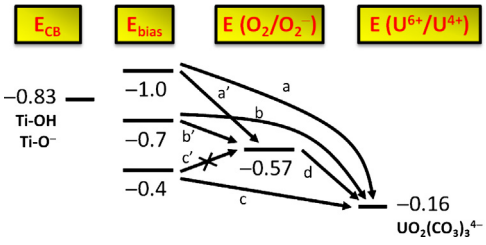

Scheme 1. Illustration for energy levels of TiO_2 conduction band (CB), potential bias (E_{bias}), and reduction potentials of dissolved oxygen and U(VI). The numbers refer to voltages with respect to saturated calomel electrode (SCE) at pH 8.2. a, b, and c refer to direct electron transfer pathways from TiO_2 to U(VI), while a′, b′, c′, and d refer to oxygen-mediated electron transfer pathways.

radical, hydrogen peroxide, and molecular oxygen (reaction (6)) [47–49].

$$HO_2 + UO_2^{2+} \rightarrow [UO_2\text{-}HO_2]^{2+} \quad k_5 = 1.5 \times 10^5\ M^{-1}\ s^{-1} \tag{5}$$

$$HO_2 + [UO_2\text{-}HO_2]^{2+} \rightarrow UO_2^{2+} + H_2O_2 + O_2 \quad k_6 = 5 \times 10^5\ M^{-1}\ s^{-1} \tag{6}$$

$$H_2O_2 + e^- \rightarrow {}^{\bullet}OH + OH^- \tag{7}$$

As long as HO_2 is continuously present, the amount of UO_2^{2+} will remain constant because reaction (6) is faster than reaction (5). Furthermore, H_2O_2 can be photoelectrochemically decomposed into hydroxyl radicals (reaction (7)), which in turn can re-oxidize the reduced uranium. The pathway of direct electron transfer from TiO_2 to U(VI) may also exist, particularly at pH 8.2. It has been postulated that the U(VI) species in seawater at pH 8.2 (e.g., $UO_2(CO_3)_3^{4-}$) makes a strong complex with TiO_2 (i.e., >Ti-O^-) in the form of (2 >Ti-O^-)—$UO_2(CO_3)_2^{2-}$ [44,45]. A direct charge transfer may occur, yet in a very limited manner because the amount of U(VI) adsorbed at pH 8.2 is very small (~1.6 ppm).

4. Conclusions

This study has demonstrated that hexavalent uranium could be removed from seawater by TiO_2 electrodes and further reduced to tetravalent uranium using simulated sunlight irradiation. Electrochemical and photocatalytic approaches have also shown to be effective, but the combination of the two approaches resulting in positive synergistic effects proved to be more promising in both the reduction and removal of U(VI) from seawater. The most remarkable finding is that the removal of U(VI) is favored by very specific conditions where dissolved oxygen plays a key role of electron shuttle between TiO_2 and U(VI). Although the direct charge transfer is thermodynamically allowed, the electrostatic repulsion between TiO_2 and bulky U(VI) species appear to hinder the transfer at the low and circum-neutral pH values. The uranium species that were removed were uniformly distributed between the TiO_2 surface and seawater. The Faradaic efficiency for the photoelectrochemical U(VI) reduction was nearly 100% at $-1.0\ V_{SCE}$. Although a high concentration of U(VI) was used in the laboratory experiments, the employed PEC-treatment technique appears to be promising because of the easy fabrication of low-cost TiO_2 electrodes and a simple experimental setup with no requirement for external electrolyte.

Acknowledgements

This research was financially supported by the Basic Science Research Programs (nos. 2012R1A2A2A01004517 and 2011-0021148), Framework of International Cooperation Program (no. 2013K2A1A2052901), Space Core Technology Development Program (2014M1A3A3A02034875) through the National Research Foundation (NRF), and the Korea CCS R&D Center (KCRC) (no. 2014M1A8A1049354) funded by the Ministry of Science, ICT & Future Planning, Korea.

Appendix A. Supplementary data

Supplementary data associated with this article can be found, in the online version, at http://dx.doi.org/10.1016/j.apcatb.2014.08.041.

References

[1] R.C. Ewing, MRS Bull. 33 (2008) 338–340.
[2] D. Cui, J. Low, K. Spahiu, Energy Environ. Sci. 4 (2011) 2537–2545.
[3] J. Kim, C. Tsouris, R.T. Mayes, Y. Oyola, T. Saito, C.J. Janke, S. Dai, E. Schneider, D. Sachde, Sep. Sci. Technol. 48 (2013) 367–387.
[4] D.L. Clark, D.E. Hobart, M.P. Neu, Chem. Rev. 95 (1995) 25–48.
[5] K. Maher, J.R. Bargar, G.E. Brown Jr., Inorg. Chem. 52 (2013) 3510–3532.
[6] IAEA, Fukushima Daiichi Status Report, Available at http://www.iaea.org/newscenter/focus/fukushima/status-reports.html, International Atomic Energy Agency, 2013.
[7] K. Kusakabe, A. Goto, S. Morooka, Sep. Sci. Technol. 29 (1994) 1567–1577.
[8] R.V. Davies, J. Kennedy, K.M. Hill, R.W. McIlroy, R. Spence, Nature 203 (1964) 1110.
[9] S. Nakamura, S. Mori, H. Yoshimuta, Y. Ito, M. Kanno, Sep. Sci. Technol. 23 (1988) 731–743.
[10] H.S. Mahal, B. Venkataramani, K.S. Venkateswarlu, J. Inorg. Nucl. Chem. 43 (1981) 3335–3342.
[11] M.J. Comarmond, T.E. Payne, J.J. Harrison, S. Thiruvoth, H.K. Wong, R.D. Aughterson, G.R. Lumpkin, K. Mueller, H. Foerstendorf, Environ. Sci. Technol. 45 (2011) 5536–5542.
[12] A. Zhang, G. Uchiyama, T. Asakura, React. Funct. Polym. 63 (2005) 143–153.
[13] B. Ahmed, B. Cao, B. Mishra, M.I. Boyanov, K.M. Kemner, J.K. Fredrickson, H. Beyenal, Water Res. 46 (2012) 3989–3998.
[14] X. Rui, M.J. Kwon, E.J. O'Loughlin, S. Dunham-Cheatham, J.B. Fein, B. Bunker, K.M. Kemner, M.I. Boyanov, Environ. Sci. Technol. 47 (2013) 5668–5678.
[15] J.D. Wall, L.R. Krumholz, Annu. Rev. Microbiol. (2006) 149–166.
[16] B. Gu, L. Liang, M.J. Dickey, X. Yin, S. Dai, Environ. Sci. Technol. 32 (1998) 3366–3373.
[17] S.P. Hyun, J.A. Davis, K. Sun, K.F. Hayes, Environ. Sci. Technol. 46 (2012) 3369–3376.
[18] R. Amadelli, A. Maldotti, S. Sostero, V. Carassiti, J. Chem. Soc., Faraday Trans. 87 (1991) 3267–3273.
[19] M. Bonato, G.C. Allen, T.B. Scott, Micro Nano Lett. 3 (2008) 57–61.
[20] M. Bonato, K.V. Ragnarsdottir, G.C. Allen, Water Air Soil Pollut. 223 (2012) 3845–3857.
[21] J. Chen, D.F. Ollis, W.H. Rulkens, H. Bruning, Colloids Surf. A 151 (1999) 339–349.
[22] V. Eliet, G. Bidoglio, Environ. Sci. Technol. 32 (1998) 3155–3161.
[23] A.G. Dickson, C. Goyet (Eds.), Handbook of Methods for the Analysis of the Various Parameters of the Carbon Dioxide System in Sea Water, Department of Energy, U.S.A., 1994.
[24] H. Park, Y. Park, W. Kim, W. Choi, J. Photochem. Photobiol. C 15 (2013) 1–20.
[25] H. Park, A. Bak, T.H. Jeon, S. Kim, W. Choi, Appl. Catal. B 115–116 (2012) 74–80.
[26] S.O. Odoh, Q.J. Pan, G.A. Shamov, F.Y. Wang, M. Fayek, G. Schreckenbach, Chem.-Eur. J. 18 (2012) 7117–7127.
[27] E. Selli, V. Eliet, M.R. Spini, G. Bidoglio, Environ. Sci. Technol. 34 (2000) 3742–3748.
[28] T.M. McCleskey, T.M. Foreman, E.E. Hallman, C.J. Burns, N.N. Sauer, Environ. Sci. Technol. 35 (2001) 547–551.
[29] M.-J. Kim, K.-H. Choo, H.-S. Park, J. Photochem. Photobiol. A 216 (2010) 215–220.
[30] S. Kim, H. Park, RSC Adv. 3 (2013) 17551–17558.
[31] M. Russo, S.E.J. Rigby, W. Caseri, N. Stingelin, J. Mater. Chem. 20 (2010) 1348–1356.
[32] S.B. Savvin, Talanta 8 (1961) 673–685.
[33] H. Rohwer, N. Rheeder, E. Hosten, Anal. Chim. Acta 341 (1997) 263–268.
[34] M.H. Khan, P. Warwick, N. Evans, Chemosphere 63 (2006) 1165–1169.
[35] T. Nakashima, K. Yoshimura, T. Taketatsu, Talanta 39 (1992) 523–527.
[36] T.M. Bhatti, A. Mateen, M. Amin, K.A. Malik, A.M. Khalid, J. Chem. Technol. Biotechnol. 52 (1991) 331–341.
[37] F. Fabregat-Santiago, I. Mora-Sero, G. Garcia-Belmonte, Y. Bisquert, J. Phys. Chem. B 107 (2003) 758–768.
[38] U. Kang, H. Park, Appl. Catal. B 140-141 (2013) 233–240.
[39] C. Hennig, A. Ikeda-Ohno, F. Emmerling, W. Kraus, G. Bernhard, Dalton Trans. 39 (2010) 3744–3750.
[40] M. Sutton, S.R. Burastero, Chem. Res. Toxicol. 17 (2004) 1468–1480.
[41] H. Ervanne, S. Puukko, M. Hakanen, Modeling of Sorption of Eu, Mo, Nb, Ni, Pa, Se, Sn, Th and U on Kaolinite and Illite in Olkiluoto Groundwater Simulants, Posiva, Olkiluoto, 2013.
[42] M.S. Vohra, S. Kim, W. Choi, J. Photochem. Photobiol. A 160 (2003) 55–60.
[43] C.H. Ho, D.C. Doern, Can. J. Chem. 63 (1985) 1100–1104.
[44] N. Jaffrezic-Renault, H. Andrade-Martins, J. Radioanal. Chem. 55 (1980) 307–316.
[45] Z. Wang, S.-W. Lee, J.F. Catalano, J.S. Lezama-Pacheco, J.R. Bargar, B.M. Tebo, D.E. Giammar, Environ. Sci. Technol. 47 (2013) 850–858.
[46] H. Park, W. Choi, J. Phys. Chem. B 108 (2004) 4086–4093.
[47] B.H.J. Bielski, D.E. Cabelli, R.L. Arudi, J. Phys. Chem. Ref. Data 14 (1985) 1041–1100.
[48] D. Meisel, Y.A. Ilan, G. Czapski, J. Phys. Chem. 78 (1974) 2330–2334.
[49] D. Meisel, G. Czapski, A. Samuni, J. Am. Chem. Soc. 95 (1973) 4148–4153.